

Application of the Generalized Gamma Model to Represent the Full DSD Spectra

Merhala Thurai, and V. N. Bringi

Dept. of ECE, Colorado State University, Fort Collins, Colorado, USA

1. Introduction

Drop size distribution data from two collocated disdrometers (Meteorological Particle Spectrometer and 2D-video disdrometer) from recent measurement campaigns (Thurai et al., 2017), in Greeley, CO, and Huntsville, AL, have revealed that the full DSD spectra (at hourly and 5-min averages) can be represented by a combination of (i) a drizzle mode for drop diameters less than around 0.7 mm and (ii) a precipitation mode starting around 0.7-1 mm region, i.e. the ‘shoulder’ region, and extending to larger sizes. The two modes tended to be more prominent (at the hourly averaging) for the Huntsville cases relative to the Colorado events reflecting the climatological differences between the two locations.

Our new results point to the potential need for additional work on modeling the full DSD spectra. In this paper, we consider the formulation given in Lee et al. (2004), in particular the scaling form of the generalized gamma DSD with the 4 parameters namely: generalized characteristic number density, N_0' , the generalized characteristic diameter, D_m' and two ‘shape’ parameters c and μ .

Such formulation has been tested using our measurements of the full DSD spectra. Initial results are promising. 3 minute sample DSD measurements from both locations show good fit to the data at both the small and large drop ends, simultaneously. The standard 3-parameter gamma model (which is a special form of generalized gamma formulation) was unable to provide such good fits at both the small and large drop ends.

We present here illustrative case examples, both from Greeley and from Huntsville and compare the characteristics of these events in both locations in terms of the variability of the 4 generalized gamma DSD parameters. Events range from light precipitation to convective storms.

2. Model Testing

Testing of the generalized gamma model was done following the same equation (43), as in Lee et al. (2004), as given below in eq. (1):

$$N(D) = N_0' h_{GG(i,j,\mu,c)} \left(\frac{D}{D_m'} \right) \quad (1)$$

$$\text{where } N_0' = M_i^{(j+1)/(j-i)} M_j^{(i+1)/(i-j)} \quad \text{and} \quad D_m' = (M_j / M_i)^{1/(j-i)}$$

and

$$h_{GG(i,j,\mu,c)} = c \Gamma_i^{\frac{(j+c\mu)}{(i-j)}} \Gamma_j^{\frac{(-i-c\mu)}{(i-j)}} x^{c\mu-1} \exp\left[-\left(\frac{\Gamma_i}{\Gamma_j}\right)^{\frac{c}{(i-j)}}\right] x^c$$

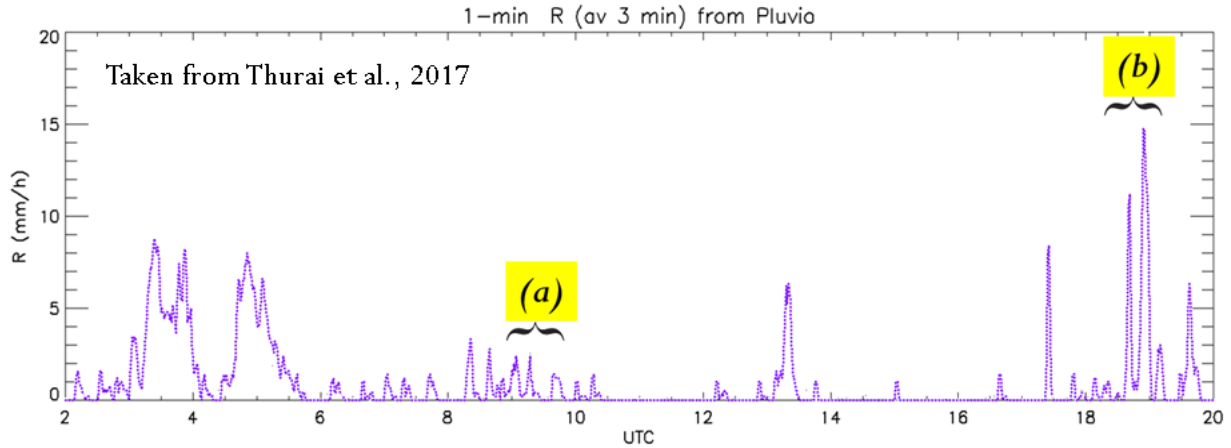
$$\Gamma_i = \Gamma\left(\mu + \frac{i}{c}\right) \text{ and } \Gamma_j = \Gamma\left(\mu + \frac{j}{c}\right)$$

$$x = \left(\frac{D}{D_m'}\right)$$

Setting $i = 3$ and $j = 4$, a global fitting of c and μ was performed by minimizing the squared difference on log scale. The measured DSD spectra (over 3 minutes) which are used as input

to the fitting procedure were constructed by utilizing the corresponding MPS-based $N(D)$ measurements for $0.15 < D_{eq} \leq 1$ mm and the 2DVD-based DSD measurements for $D_{eq} > 1$ mm.

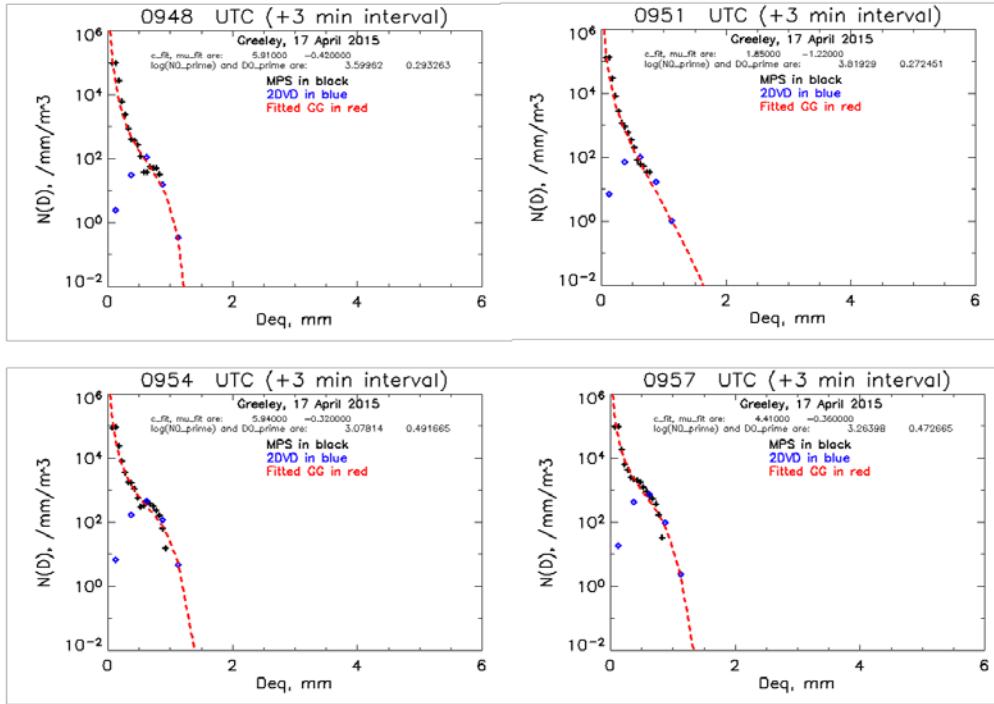
2.1 First set of examples: selected periods from the 17 April 2015 event at Greeley, Colorado



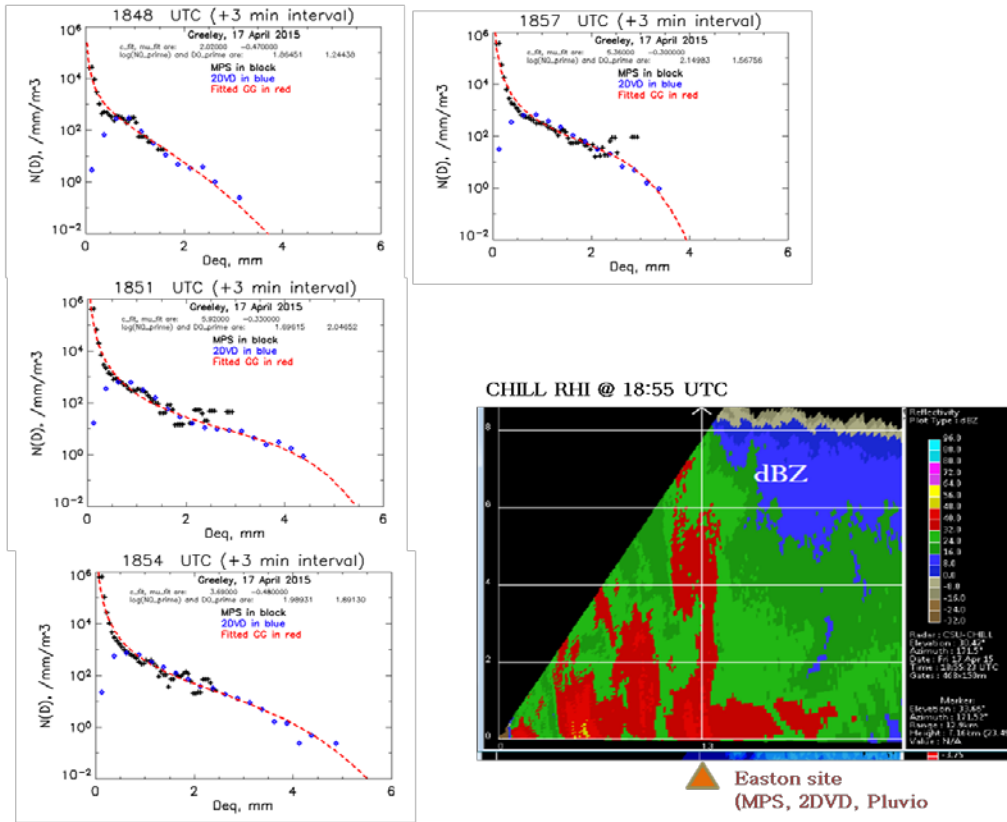
Period (a) corresponds to ‘light precip’ event and period (b) corresponds to convective storm at the disdrometer site. (Thurai et al., 2017). Results are shown below. Note, the measured DSDs both from the MPS (in black) and the 2DVD (in blue)

are shown for the entire D_{eq} range. The fitted curve is represented by the red dotted lines, and the fitted parameters of μ and c are shown in each panel, together with $\log_{10}(N_0')$ and D_m' values.

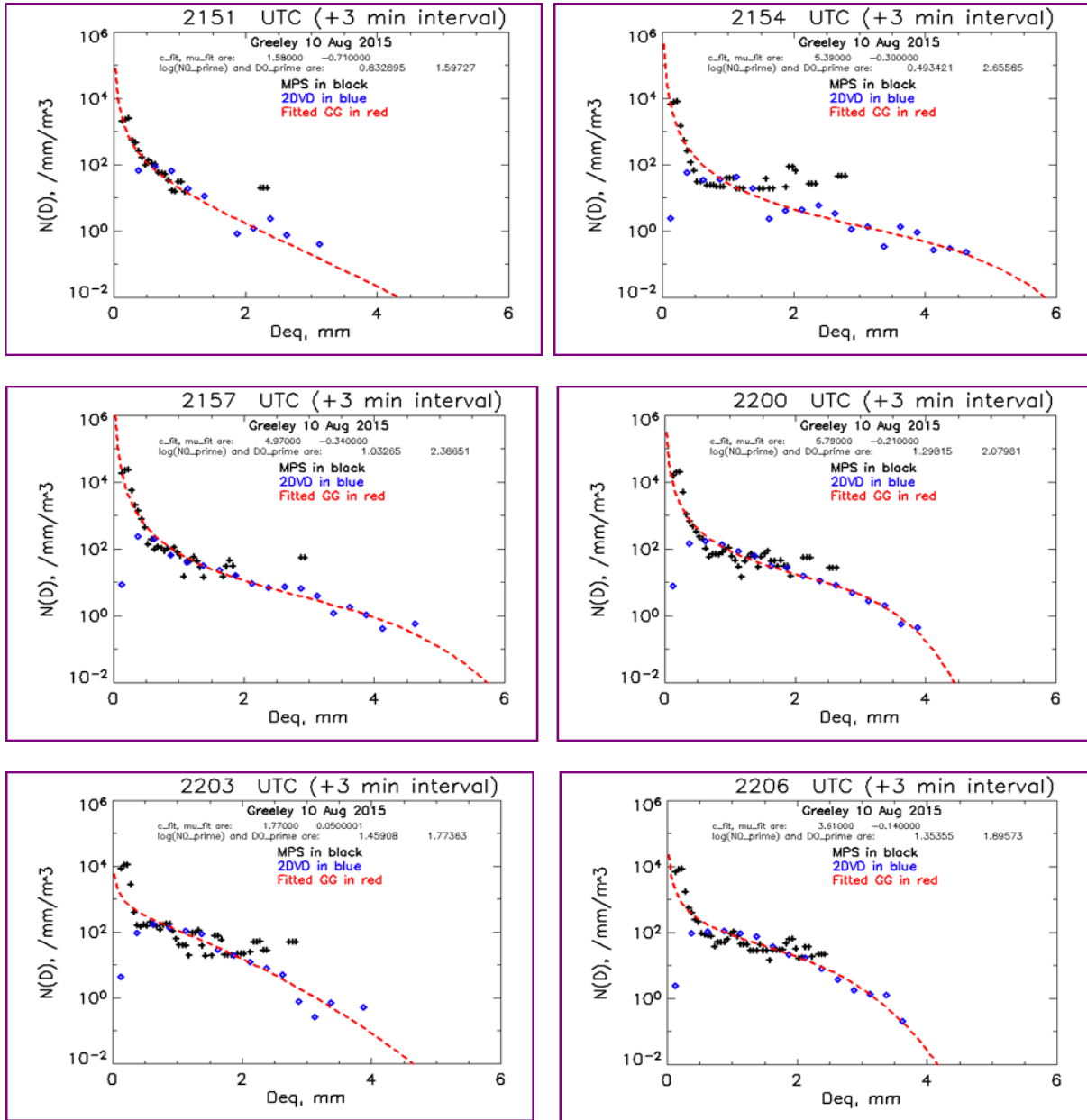
(a) Light Precip



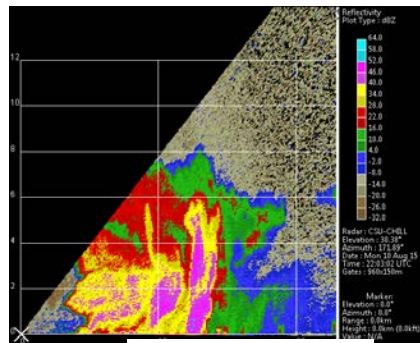
(b) Convective storm



2.2 **Second set of examples:** selected periods from the 10 Aug 2015 convective event at Greeley

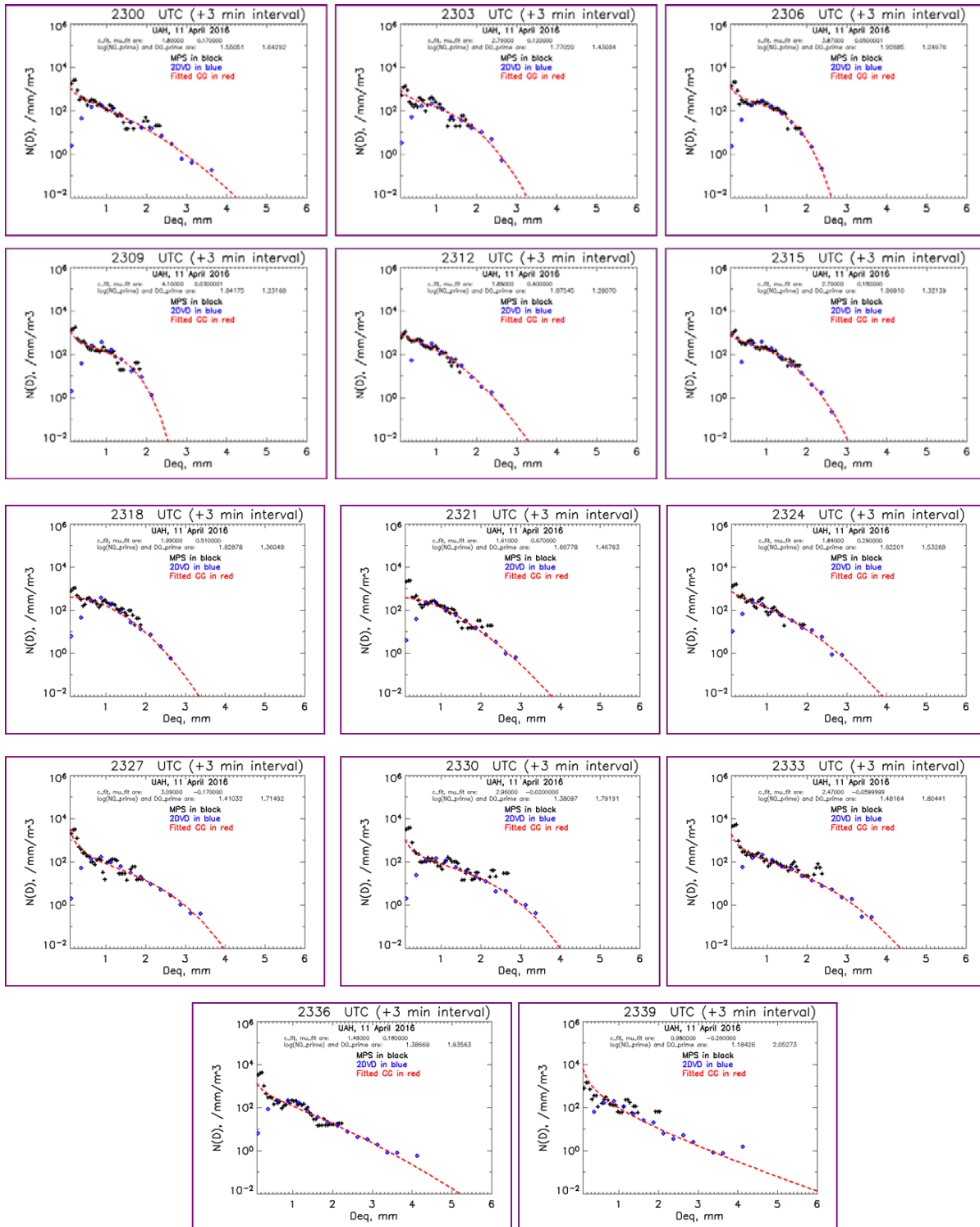


CHILL RHI at 22:03 UTC

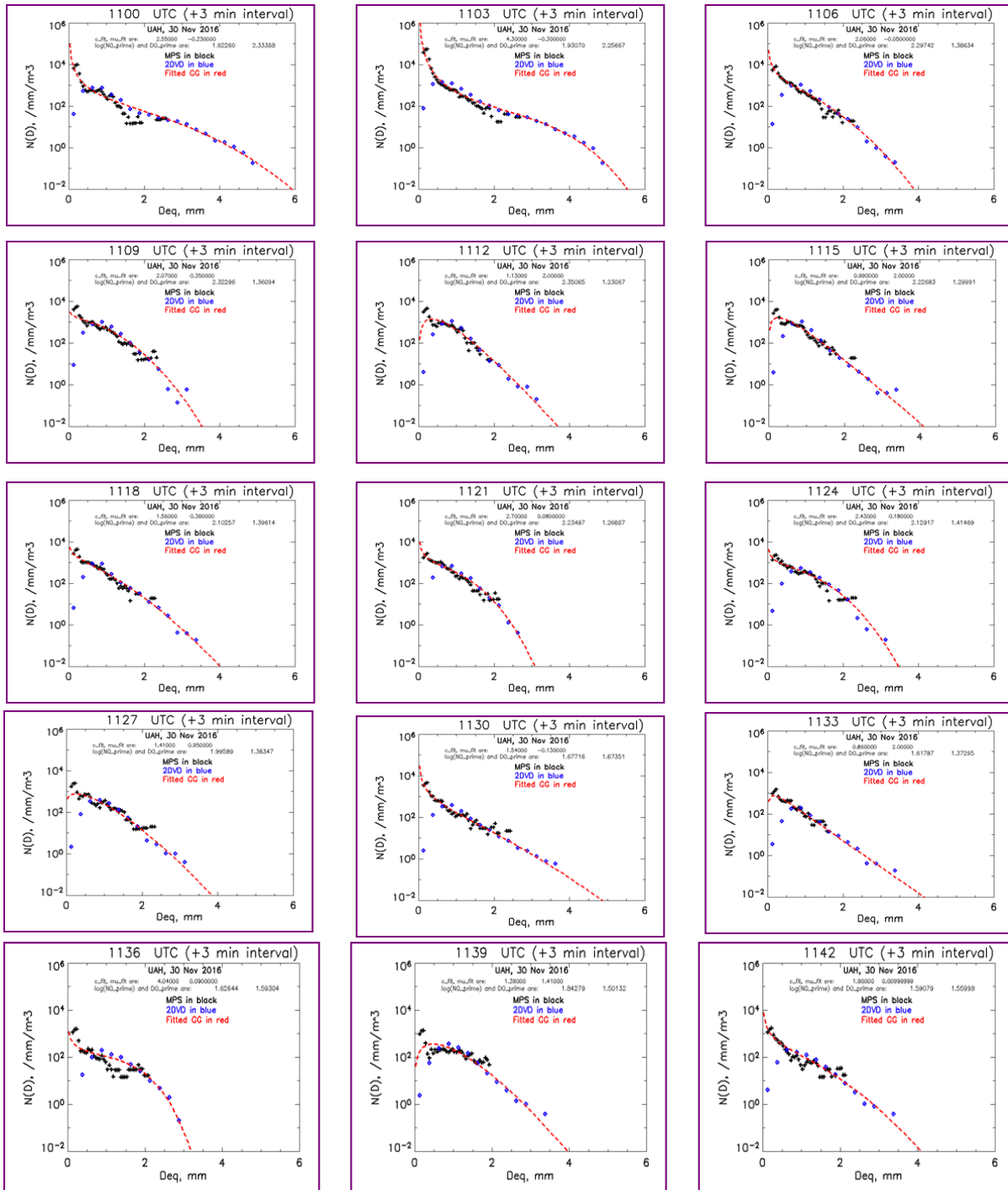


↑ MPS, 2DVD

2.3 Third set of examples: around the GPM overpass time (2331 UTC) on 11 Apr 2016, Huntsville



2.4 Fourth set of examples: from an event on 30 Nov 2016, UA Huntsville (MPS was outside DFIR)



3 Variation of the fitted parameters with R

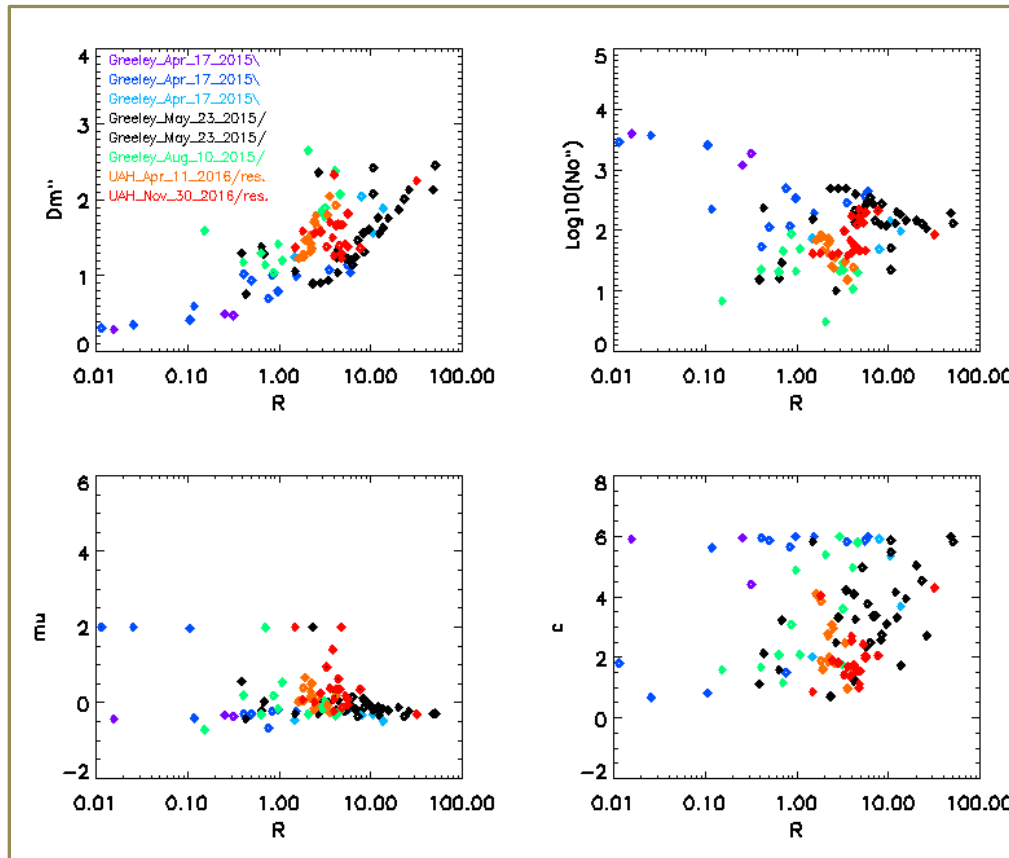
A summary of the fitted parameters for arbitrarily selected time periods during several events, both from Greeley and from Huntsville, are shown as a function of the (3-minute) rain rates in the figure below. Each color represents the different time periods or events. The top left shows the variation of D_m' , top right the variation of $\log_{10}(N_0')$, the bottom left for μ and the bottom right for the value of c .

From these plots, it appears that:

- (a) D_m' tends to increase with rain rate (expected)
- (b) Some tendency for $\log_{10}(N_0')$ to decrease with R

- (c) Values of μ tend to be close to 0 or slightly negative (high concentration of small drops). Their range is narrow.
- (d) c does not seem to be correlated with R but as given in the next section, it can have larger range of uncertainties associated with it.
- (e) For a given R, the Huntsville events appear to have higher D_m , lower $\log_{10}(N_0')$, μ values which are closer to zero or slightly positive, and somewhat lower c values. The lower c values and the high D_m indicate wider distributions towards larger drops, although when μ is slightly negative, the effect of c is much less.

Family of curves showing the effects of varying c and varying μ are shown in the Appendix.



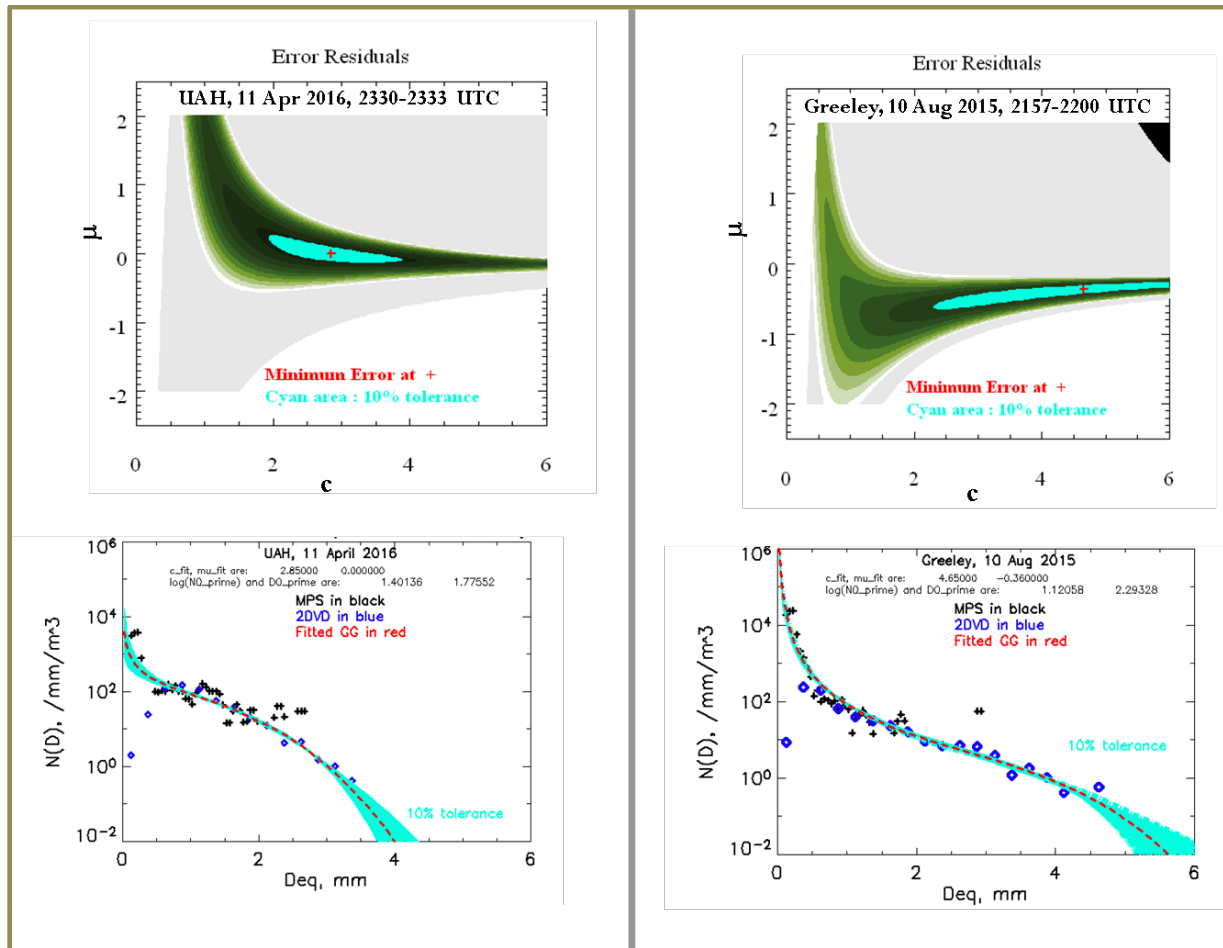
4 Error residuals

Two examples of the residual errors in $c - \mu$ space are shown as color-filled plots on the top panels of the figure below. The events correspond to (i) UAH, 11 April 2016, during the GPM overpass at around 23:31 UTC, and (ii) Greeley, 10 Aug 2015, during a convective rain event at 23:57 UTC. Both cases were shown earlier in section 2, and in both cases, the same 3-min DSDs were used for the fitting.

Darker areas in the error residual plots represent lower errors, and the “red +” points represent the lowest error. And highlighted in cyan color are the areas where the errors were less than 10% of the minimum error. While the cyan areas span

only a very limited range in μ values, in terms of c values, they extend to larger ranges. In the UAH event case, c ranges from 2 to 4; for the Greeley case, the range is even larger, extending from 2 to 6.

The fitted curves with the corresponding 10% error tolerance are shown in the two bottom panels (red – minimum error; cyan – to within 10% of minimum error). For the UAH case (stratiform rain), the ‘flare’ occurs at both the small drop end and the large drop end. By contrast, for the Greeley case (convective rain), the flare occurs only at the large drop end (sampling issues may play a role here). For the medium-sized drops, the effect is hardly noticeable, for both events.



5 Conclusions

Testing of eq. (1) against our datasets of the composite MPS-2DVD DSDs has highlighted the suitability of this formulation to represent the full spectra. Analysis of error residuals has indicated that although minim error can be reached in the $c - \mu$ domain, if one allows 10% error tolerance then c can vary over a significant range. μ on the other hand appears to be a more sensitive parameter, and lies within a narrow range

Acknowledgements

We wish to thank Pat Kennedy (CSU-CHILL) for performing CHILL radar scans for selected events during the Greeley campaign (April to Oct 2015), as well as Patrick Gatlin, Larry Carey, Walter Petersen, for hosting the MPS and the 2DVD instruments at the UA Huntsville site, and for the helpful discussions. We also appreciate help from Wonbae Bang (c/o Prof. G. Lee at KNU, Daegu, ROK) for some initial help with the fitting procedure.

We acknowledge support by the US National Science Foundation under Grant AGS-1431127. Additionally MT acknowledges support from NASA's Global Precipitation Measurement program through Award NNX16AD47G.

References

Lee, G., I. Zawadzki, W. Szyrmer, D. Sempere-Torres, and R. Uijlenhoet, 2004: 'A general approach to double-moment normalization of drop size distributions', *J. Appl. Meteor.*, **43**, 264–281

Thurai, M. P. Gatlin, V. N. Bringi, W. Petersen, P. Kennedy, B. Notaroš, and L. Carey, 2017: 'Toward Completing the Raindrop Size Spectrum: Case Studies Involving 2D-Video Disdrometer, Droplet Spectrometer, and Polarimetric Radar Measurements', *J. Appl. Meteor. Climatol.*, **56** (4), 877–896.

Related References

Auf der Maur, A. N., 2001: Statistical tools for drop size distribution: Moments and generalized gamma. *J. Atmos. Sci.*, **58**, 407–418.

Field, P. R., R. J. Hogan, P. R. A. Brown, A. J. Illingworth, T. W. Choullarton, and R. J. Cotton, 2005: Parametrization of ice-particle size distributions for mid-latitude stratiform cloud. *Quart. J. Roy. Meteor. Soc.*, **131**, 1997–2017.

Raupach, T.H. and A. Berne, 2017: Invariance of the Double-Moment Normalized Raindrop Size Distribution through 3D Spatial Displacement in Stratiform Rain. *J. Appl. Meteor. Climatol.*, **56**, 1663–1680

Appendix: Effects of varying c and μ on the DSDs

The left panels below show the effect of μ on DSDs when c is fixed 1, 2, and 3. The right panels show the effect of c when μ is fixed at -0.1, 0 and 1. In all cases, N_0' was set to 10^2 /mm/m³, and D_m' to 1.5 mm.

In general, when c is fixed, the effect of μ is to adjust the width at the DSD spectra at both ends;

specifically, lower μ values will extend the spectra at both ends. On the other hand, the effect of c will depend on the value of μ . When μ is -0.5, c has less effect (no trend is visible) compared with when μ is 1. When μ is close to 0, c shows more effect at the large drop end; lower values of c extend the spectra to higher concentrations of larger drops (in relative terms).

